

Dissection of the target specificity of the RNA-binding protein HOW reveals *dpp* mRNA as a novel HOW target

David Israeli, Ronit Nir and Talila Volk*

Regulation of RNA metabolism plays a major role in controlling gene expression during developmental processes. The *Drosophila* RNA-binding protein Held out wing (HOW), regulates an array of developmental processes in embryonic and adult growth. We have characterized the primary sequence and secondary structural requirements for the HOW response element (HRE), and show that this site is necessary and sufficient for HOW binding. Based on this analysis, we have identified the *Drosophila* TGF β homolog, *dpp*, as a novel direct target for HOW negative regulation in the wing imaginal disc. The binding of the repressor isoform HOW(L) to the *dpp* 3' untranslated region (UTR) leads to a reduction of *GFP-dpp* 3' UTR reporter levels in S-2 cells, in an HRE site-dependent manner. Moreover, co-expression of HOW(L) in the wing imaginal disc with a *dpp-GFP* fusion construct led to a reduction in DPP-GFP levels in a *dpp*-3' UTR-dependent manner. Conversely, a reduction of the endogenous levels of HOW by targeted expression of HOW-specific double-stranded RNA led to a corresponding elevation in *dpp* mRNA level in the wing imaginal disc. Thus, by characterizing the RNA sequences that bind HOW, we demonstrate a novel aspect of regulation, at the mRNA level, of *Drosophila* DPP.

KEY WORDS: RNA, DPP, *Drosophila*, Wing imaginal disc, STAR proteins

INTRODUCTION

The control of RNA metabolism is mediated by conserved mechanisms that are fundamental to the development of multicellular organisms (de Moor et al., 2005; Kuersten and Goodwin, 2003; Lasko, 2003). The highly conserved STAR (signal transduction and activation of RNA) family includes RNA-binding proteins that control a wide variety of developmental processes, including the transition from mitosis to meiosis and sex determination by GLD-1 in *Caenorhabditis elegans* (Crittenden et al., 2003; Lee and Schedl, 2001); mesoderm, heart and tendon development by Held out wing (HOW) in *Drosophila* (Baehrecke, 1997; Lo and Frasch, 1997; Nabel-Rosen et al., 1999; Nabel-Rosen et al., 2002; Nabel-Rosen et al., 2005; Zaffran et al., 1997), and central and peripheral nervous system myelination by quaking (QKI) in mice (Ebersole et al., 1996; Li et al., 2000). STAR family members share a single conserved enlarged heterogeneous nuclear ribonucleoprotein (hnRNP) K homology (maxi-KH) RNA-binding domain flanked by two additional highly conserved domains, QUA1 and QUA2 (Vernet and Artzt, 1997), which are conserved from *C. elegans* to humans.

Studies on the *C. elegans* protein GLD-1 revealed that a single STAR protein may regulate a large number of target mRNAs, thereby simultaneously mediating the transition between distinct differentiation states in a given tissue (Crittenden et al., 2003; Lee and Schedl, 2001). Recently, a consensus hexanucleotide sequence, UACU(C/A)A, was reported to represent the actual GLD-1-binding site on its target RNA, *tra-2* (Ryder et al., 2004). It was reported that GLD-1 has the highest affinity for the sequence UACUCA. These studies were extended to show that a similar but not identical sequence, NA(A>C)UAA, represents the quaking response element

(QRE) in mouse (Ryder and Williamson, 2004; Galarneau and Richard, 2005). The partial similarity between GLD-1 and quaking response elements suggests that the extended conserved KH domain of STAR proteins recognizes common RNA sequences.

In this study, we characterized the nucleotide sequence of the *Drosophila* HOW response element (HRE) and identified secondary structure constraints that further regulate HOW binding. Based on these criteria, we identified *dpp* as a novel putative target for HOW regulation in the wing imaginal disc. Consistently, overexpression of the repressor isoform of HOW, HOW(L), reduced *dpp* mRNA levels, as well as DPP-GFP fusion-protein levels. In addition, reducing HOW levels in the wing imaginal disc led to an elevation in *dpp* mRNA levels. These experiments reveal a novel post-transcriptional regulation of DPP in the wing imaginal disc mediated by the RNA-binding protein HOW.

MATERIALS AND METHODS

Fly strains

We used the following fly strains: FRT82B*how^{stru}/TM6*; *scalloped(sd)-gal4*; *dpp-gal4*; UAS-*GFP*; *vg-gal4*; *ap-gal4*; *ms1096-gal4* (Bloomington stock center); *hs-flp*; FRT82B, μ Myc,Minute(3R)w124/TM2 (K. Basler, University of Zurich, Zurich, Switzerland); HOW(L), ds-HOW(L), and ds-HOW (produced in our laboratory); DPP-GFP without its 3' untranslated region (UTR) (S. Cohen, EMBL, Germany); DPP-GFP with its 3' UTR (M. Gonzalez-Gaitan, Dresden, Germany).

Imaginal disc labeling

The following primary antibodies were used: anti-HOW (produced in our laboratory); anti-Spalt major (A. Salzberg, Technion, Haifa); and anti-Engrailed (Hybridoma Stock Center). A mixture of three digoxigenin (DIG)-DNA labeled probes for *dpp* mRNA were produced using PCR DIG labeling mix (Roche).

Protein-RNA binding assay

Protein-RNA binding assays were performed essentially as previously described (Nabel-Rosen et al., 1999). The biotin-labeled RNA was purified on a G-50 Sephadex Quick Spin Column (Roche) and then mixed with equal amounts of in vitro-translated (TNT T7 quick coupled transcription/translation system, Promega) HOW(L) or HOW(L)^m

Department of Molecular Genetics, Weizmann Institute of Science, Rehovot 76100, Israel.

*Author for correspondence (e-mail: lgvolk@weizmann.ac.il)

(mutated) hemagglutinin (HA)-tagged proteins were added to the RNA (final concentration of RNA in each sample was 0.4 μ M). The RNA was then precipitated with magnetic streptavidin-coupled beads. The magnetic beads were then isolated, washed and boiled in sample buffer, and the supernatant was analyzed by western blot analysis with anti-HA antibodies (1:2000 dilution). HOW(L)-TAP is a fusion protein containing a tandem affinity purification (TAP) tag at the C-terminus of HOW(L).

Transient transfection of S-2R+ cells

S-2R+ cells were grown in Schneider's medium supplemented with 10% fetal calf serum (Hyclone) and 1% pen-strep solution. For transfection, cells were seeded at $3.5\text{--}5 \times 10^6$ cells in 4.5 ml medium per 50 ml flask (Nunc) and allowed to adhere. Transfection was performed using lipid reagent, according to the manufacturer's protocol (Escort IV, Sigma). A total of 6 μ g DNA was used for each transfection. Cells were collected for analysis 48 hours after transfection.

Primers used to construct the various RNA fragments

PCR was performed with Pwo DNA polymerase (Roche), using the cDNA of *stripe*, and *dpp*. The following primers were used to create the PCR fragments (all 5' primers included an additional T7 sequence): Sr1, 5'-AGACTAGAGGAGAAGTCCGGCATC-3'; Sr254, 5'-AGAGCTCATCCGGAAAGCAA-3'; Sr610, 5'-TCTAATACTGTGATCTCC-3'; Sr657, 5'-TTACATAACTGCAAGTAACC-3'; Sr885, 5'-CGAACACACACACAAATCTT-3'; Sr253, 5'-ACTTCTCCTGGACGCTGACG-3'; Sr504, 5'-TTCGATTCTTGATCTCTT-3'; Sr533, 5'-TTGTATGGTATGTAAGTCTG-3'; Sr630, 5'-ATGGAGATCACAGTATTAGA-3'; Sr770, 5'-TTAGTGTGTGTGTTTCGT-3'; Sr912, 5'-CTGATATGCTAAGATTGTG-3'; Sr1251, 5'-TGCAAGGTAAAGTAAACTAA-3'; Dpp1, 5'-ATTCGCACCACCATCGCACC-3'; Dpp1020, 5'-CTGAGCTTACGCGTTAGGTC-3'; Dppcds10, 5'-TGGCTTCTACTCCTCGCAGTG-3'; Dppcds412, 5'-TCCTTGACAGCCATTTTGTG-3'; Dppcds766, 5'-GCTTCTTCATCGGCTCGGGGA-3'; Dpp3utr424, 5'-GCTGCTGAAAGGAGAAGTTAAG-3'.

Primers for stable structures

The following primers were used: Sr_225+loop11, 5'-CCCCGGTTT-AGTATGTGCCGGGGGTAGAAGAAGGGCTGACTGG-3'; Sr_225+loop12, 5'-CCCCGGTTT-AGTATGTGCCGGGGGTAGAAGAAGGGCTGACTGG-3'; Sr_225+loop13, 5'-CCCCGGTTT-AGTATGTGCCGGGGGTAGAAGAAGGGCTGACTGG-3'; Sr_225+loop14, 5'-CCCCGGTTT-AGTATGTGCCGGGGGTAGAAGAAGGGCTGACTGG-3'.

Primers for mutant *stripe* (*sr*) fragments

All primers are 5' to 3', as indicated: Sr_533_ACUGA, 5'-TTGTATGGTCAGTAACTCTGTTTTGTTT-3'; Sr_533_ACUAC, 5'-TTGTATGGTAGTAACTCTGTTTTGTTT-3'; Sr_533_ACUAC, 5'-TTGTATGGTAGTAACTCTGTTTTGTTT-3'; Sr_770_ACUCC, 5'-GGAGTGTGTGTTTCGT-3'.

Mutagenesis of single nucleotides in *stripe* and *dpp* 3'UTR

To create point mutations in the 3'UTRs of *stripe* (*sr*) and *dpp*, we used Quickchange site-directed mutagenesis (Stratagene): Sr525mutF, 5'-CAAAACAGAGTTACTACCCATACAAAGCCTAAC-3'; Sr525mutR, 5'-GTTAGGCTTTGTATGGGTAGTAACTCTGTTTTG-3'; Sr543mutF, 5'-ACTAACCATAAAAGCCTAACTCAAGCAAATTGATTGATTAC-3'; Sr543mutR, 5'-GTAATCAATCAATTTGCTTGAGTTAGGCTTTGTATGGTTAGT-3'; Sr565mutF, 5'-AATTGATTGATTACTACCTATATTCGATGTAAT-3'; Sr565mutR, 5'-ATTACATCGAATATAGGTAGTAAATCAATCAATT-3'; Sr769mutF, 5'-CACACAAACACTCATTTATTGCATT-3'; Sr769mutR, 5'-AATGCAATAAATGAGTGTGTTGTGTG-3'; Dpp766mutF, 5'-CTCTCTGTATATGTACTACACACCTATATACCTTATATGCG-3'; Dpp766mutR, 5'-CGCATATAAAGTATATAGGTGTGTAGTACATACAAGAGAG-3'; Dpp882mutF, 5'-TTCGTGCGCAATCAACTACAGTAACTGTATAAACA-3'; Dpp882mutR, 5'-TTTTGTTTATACAGTTACGTGTAGTTGAATGCGCAACGAA-3'. The sequence of all PCR fragments were verified before performing the transcription reaction.

The following biotin-labeled RNA nucleotides were synthesized by IDT (IA, USA): 12 nucleotides (nt) without HRE, 5'-ACACACACACAC-3'; 12 nt with HRE, 5'-ACAUACUAACAC-3'; stem, 5'-GUUUACUAAAUGUGGUUUUAGUAAAAC-3'; loop, 5'-CCCCGGGCACATACACTAACACACCGGGGG-3'; junctional UAC, 5'-CCCUACUAAACACGGACAACGUAGGGG-3'; junctional UA, 5'-CCCUACUAAACACGCCCUAGGGG-3'; unstructured, 5'-CUACUACCCCAACC.

Construction of the HOW and HOW(L) double-stranded RNA (dsRNA) was in pWiz using the following primers: HL3utr572, 5'-ATCCTCTAGAAAAGTCAGATATCCTGAGCC-3'; HL3utr1179, 5'-ATCCTCTAGAAATAGACTTCGTGCACAATCC-3'; howcds7, 5'-ATCCTCTAGATGTCTGTGAGAGCAAAGCCG-3'; howcds519, 5'-TACCTCTAGAGCCGGTCTCCTGTTCCAATT-3'.

RESULTS

Identification of HOW-binding sites in the 3'UTR of *stripe*

Previously, we have shown that HOW binds directly to the 3'UTR of *stripe* (Nabel-Rosen et al., 1999). To characterize the HOW-binding sites further, we truncated the *stripe* 3'UTR 1.2 kb sequence into smaller fragments, which were individually transcribed in vitro and labeled with biotin. These fragments were tested for HOW binding by adding in vitro-translated HOW tagged with hemagglutinin (HA) to the biotin-labeled RNA followed by precipitation of the RNA complexes using avidin-conjugated magnetic beads. The presence of HOW on the beads was then tested by western blot analysis using anti-HA antibodies. As a control for non-specific binding, we used a mutant HOW variant (HOW^m), which carries a mis-sense mutation in the KH domain exchanging arginine at position 185 to cysteine, mimicking the severe loss-of-function *how*^{e44} allele. Previously, we showed that HOW^m does not exhibit RNA-binding activity (Nabel-Rosen et al., 2002). This analysis (not shown) allowed us to select two HOW-binding fragments (*a* and *b*) in which we identified the sequence ACUAA, which was similar, but not identical, to the GLD-1 hexanucleotide-binding site in *tra-2* (Ryder et al., 2004). In fragment *a*, there are three repeats of this sequence, and fragment *b* contains one such sequence (see Fig. 1A).

To address whether the sequence ACUAA is sufficient for HOW binding, we synthesized two RNA fragments corresponding to regions *a* or *b* that contained a single pentanucleotide ACUAA sequence and tested their binding to HOW protein. Although both fragments bound HOW, point mutations altering the ACUAA motif at position 521 to either ACUCA or ACUGA abrogated HOW binding (Fig. 1A, only fragment *a* is shown). Mutating all of the four ACUAA sites within the context of the entire *stripe* 3'UTR essentially abrogated the binding of HOW (Fig. 1B). Importantly, an RNA fragment containing all three HRE sites in a single fragment showed enhanced binding to HOW (Fig. 1C), suggesting that multiple HRE sites contribute to an elevated level of binding to this protein.

We conclude that the sequence ACUAA represents the primary HRE. Importantly, one of the HRE sequences (at position 766) is conserved in the 3'UTR of *stripe* in *Drosophila pseudoobscura*. Moreover, we identified three repeats of the pentamer AAUAA (which also binds HOW, but to a lesser extent: D.I. and T.V., unpublished data) that are conserved between the two *Drosophila* species. Thus, we show that the HOW-binding site NA(C>A)UAA closely resembles that of STAR proteins from other species, although it is not identical. We extended our understanding of the binding of STAR proteins to their targets further by examining the binding of HOW in the context of the entire *stripe* 3'UTR and demonstrated that deletion of these four sites indeed abrogates the responsiveness of the *stripe* 3'UTR to HOW (Fig. 1B).

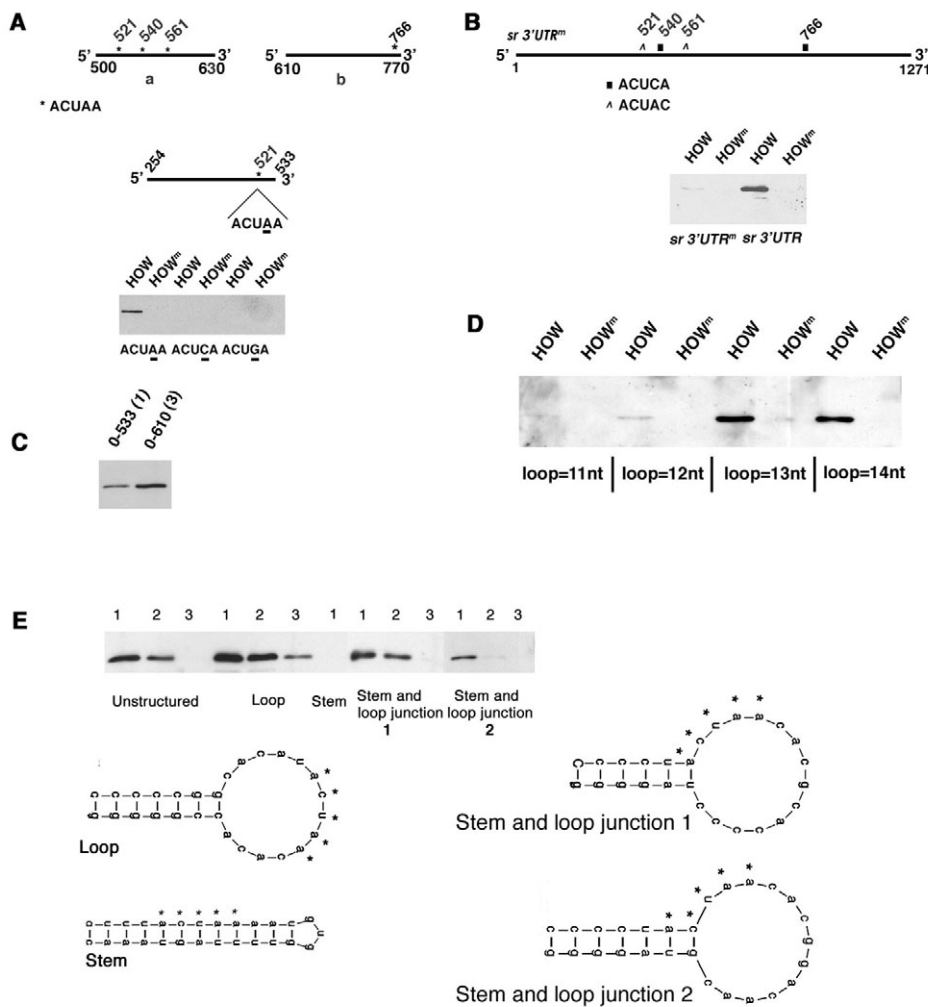


Fig. 1. Characterization of the HOW response element. Western blot analysis of HA-tagged HOW following precipitation with distinct biotin-labeled RNA fragments. **(A)** Top, schematic representation of the putative HOW response element (HRE) sites in the *stripe* 3'UTR. Bottom, the sequences of the HRE sites in the RNA samples (at 0.4 μ M concentration) are indicated below the blot; wild type (ACUAA, left) or with point mutations in the HRE site (A \rightarrow C, middle or A \rightarrow G, right). HOWtm was used as a control for non-specific binding because it mimics the *how*^{e44} allele, which does not bind RNA. **(B)** The wild-type *stripe* 3'UTR (0.4 μ M) (two right-hand lanes) or the *stripe* 3'UTR with point mutations in all four HRE sites (two left-hand lanes). **(C)** Binding of HOW to RNA fragments (0.4 μ M) representing 0-533 nucleotides of the *stripe* 3'UTR (0 represents the last nucleotide of the stop codon), containing a single HRE site (1), or representing nucleotides 0-610, containing three HRE sites (3). **(D)** HRE in loop structures of variable sizes (loop sizes are indicated) fused to the 1-225 nucleotide (nt) RNA fragment of *stripe* 3'UTR (0.4 μ M). **(E)** Biotin-labeled RNA oligomers containing a single HRE within the distinct secondary-structure motifs; unstructured, loop, stem, stem and loop junction 1, and stem and loop junction 2 (illustrated below) at concentrations of 0.2 μ M (1), 0.02 μ M (2), 0.002 μ M (3). *Indicates the HRE.

HOW binds to an HRE embedded within a loop secondary structure

Because a pentanucleotide sequence would be relatively abundant within the 3'UTRs of many RNAs, we suspected that additional restrictions might exist in addition to the primary sequence ACUAA. Analysis of the distinct HOW-binding sites in the *stripe* 3'UTR using the Mfold program (Mathews et al., 1999; Zuker, 2003) showed that high-affinity binding for HOW occurs when the binding site (ACUAA) is included within a single-stranded loop. However, secondary-structure predictions of large RNA fragments (larger than 30-40 nucleotides) using the Mfold program resulted in numerous alternatives. To test whether a loop secondary structure is essential for the binding of HOW, we constructed HRE-containing loops of distinct sizes fused to the 3' end of the *stripe* 3'UTR fragment (1-225), which does not bind HOW (Fig. 1A). We found that single-stranded loops that are larger than 12 nucleotides and contain a single HRE site exhibited significant binding, whereas loops smaller than 12 nucleotides did not exhibit specific binding to HOW (Fig. 1D). Presumably, these loops are too small to allow this binding.

To test further the contribution of the loop secondary structure for the binding of HOW, we used short RNA oligomers (26-30), which were labeled at their 5' end with biotin. The secondary-structure predictions of these oligomers by Mfold resulted in a single predicted structure, enabling us to directly test for a possible link between secondary structure and the binding of HOW. We compared the

binding of HOW to five oligomers that contained a single HRE: a single-stranded RNA oligomer that does not form any secondary structure, an oligomer that forms a loop structure, a stem-forming oligomer, an oligomer in which the HRE site starts at the junction between the stem and the loop, and an oligomer in which the two first nucleotides (AC) are on the stem and the three consecutive nucleotides (UAA) are on the loop. All oligomers contained a single copy of the HRE sequence and were labeled at the 5' end by a single biotin molecule. This analysis indicated that the RNA oligomer containing the HRE within a loop secondary structure exhibited binding to HOW at lower concentrations relative to the single-stranded RNA oligomer. Importantly, a graded reduction in HOW-binding intensity was detected as the HRE site was moved from the loop to the junction between the loop and the stem, and further towards the stem (Fig. 1E). This suggests that an HRE within a loop contributes to HOW affinity to the HRE. When the HRE was embedded within a stem structure, it did not bind to HOW (Fig. 1E). A control RNA oligomer lacking the HRE did not bind to HOW under similar conditions (data not shown). An oligomer containing the quaking-binding site (AAUAA) did show binding to HOW, although with a lesser affinity (data not shown). Similarly, we found that quaking bound to the same oligomers that proved positive for the binding of HOW, namely the unstructured oligomer, the loop oligomer, and the stem and loop junction oligomer, whereas it did not bind the RNA that contained the HRE on the stem (data not shown).

This analysis demonstrates that the secondary structure of the HRE site affects the binding specificity and that a proper secondary structure of the RNA containing the ACUAA sequence is essential for maintaining high-affinity binding of HOW to its target mRNA.

Large *how* mutant clones broaden the Spalt domain in the wing imaginal disc

Based on the sequence and secondary structures that we defined above, we next sought to identify novel mRNA targets regulated by HOW. We focused on potential HOW-target mRNAs in the wing imaginal disc. In this tissue, the nuclear isoform HOW(L) is expressed uniformly (Fig. 2A). Previous analysis of the requirements for *how* in the development of the adult wing indicated that HOW is necessary for normal adhesion between the two epithelial layers formed during the pupal stages (Lo and Frasch, 1997; Prout et al., 1997).

To study further the requirements for *how* in the wing imaginal disc, we produced large *how* clones on a Minute background. In this setup, the *how* homozygous-mutant clones possess a growth advantage over the Minute/+ background cells, whereas the twin cells representing the homozygous Minute/Minute genotype disappear. We used the *how^{stru}* null allele, which deletes HOW protein expression, allowing us to identify homozygous *how^{stru}* mutant cells because they are not reactive with anti-HOW antibody. Analysis of these imaginal discs showed that large *how* mutant clones, covering most of the wing imaginal disc pouch, led to the formation of abnormal wing imaginal discs, in which the anterior-posterior boundaries of the centrally located Spalt domain were not sharp and the entire domain appeared enlarged (Fig. 2F). The posterior *engrailed* domain (detected by staining for the Engrailed protein) appeared normal (Fig. 2G). We calculated the width of the Spalt domain (relative to wing imaginal disc width) in the following manner: the values of the width of the Spalt domain at the most ventral region, most dorsal region and along the dorsoventral border were added and divided to the width of the entire wing imaginal disc. This calculated ratio was significantly larger in the wing imaginal discs carrying large *how* mutant clones relative to wild-type discs [1.23 ± 0.14 ($n=7$) in the mutant discs versus 0.96 ± 0.03 ($n=6$) in wild-type discs; Fig. 2, lower panel]; using the *t*-test, this difference was found to be significant ($P=0.0022$). Despite the abnormal shape of the wing imaginal disc, the enlargement of the Spalt domain suggested that Dpp, a major factor affecting Spalt expression in the wing imaginal disc, might represent a target for the repressive activity of HOW.

HOW binds the 3'UTR of *dpp* and reduces the GFP levels of a GFP-*dpp* 3'UTR reporter

Analysis of the primary and secondary structure of the *dpp* 3'UTR revealed that it contains two potential HRE sites at nucleotide positions 762 and 878 (following the stop codon) (Fig. 3A). Importantly, based on the Mfold program, these HRE sites are not contained in a stem or small-loop secondary structure, implying that they may represent active HREs. A HOW-RNA binding assay showed that HOW binds to the entire (1092 nucleotide) *dpp* 3'UTR (Fig. 3B). Point mutations in both HRE sites, changing these sites into ACUAC (instead of ACUAA) in the context of the entire *dpp* 3'UTR, essentially abrogated the binding of HOW (Fig. 3B). Thus, HOW binds to the *dpp* 3'UTR in a sequence-dependent manner.

To characterize further the activity of the HRE sites in the 3'UTR of *dpp*, we created a GFP reporter fused to the wild-type *dpp* 3'UTR or to a mutated 3'UTR, in which the two HRE sites were mutated

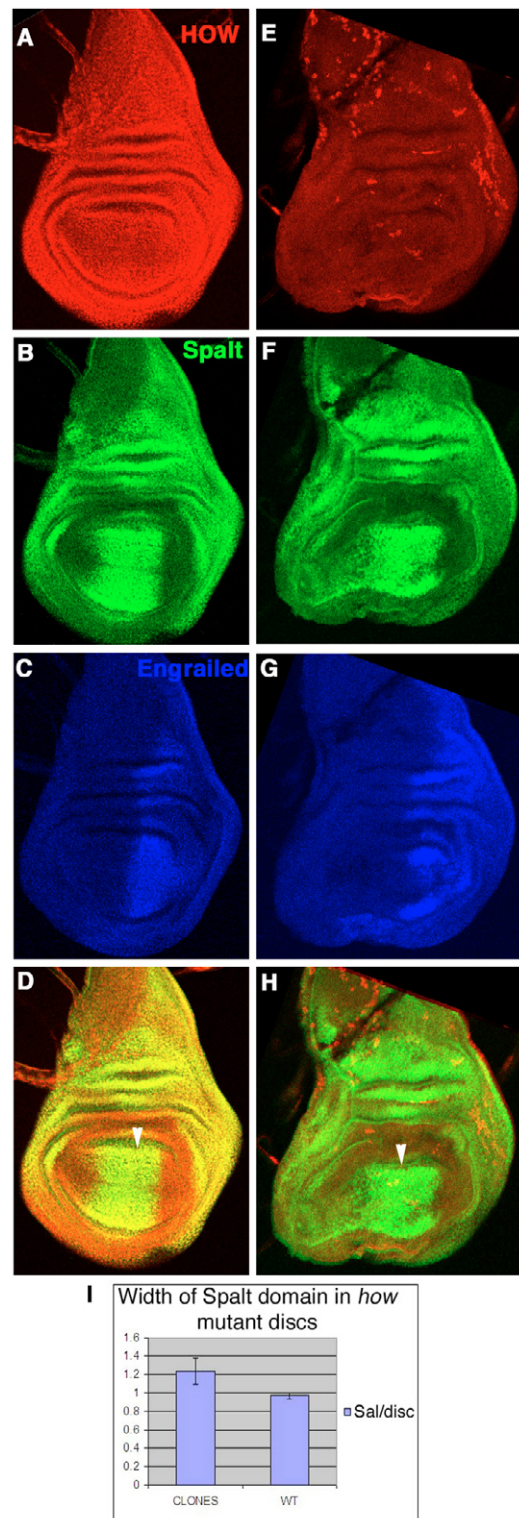


Fig. 2. Large *how^{stru}* mutant clones exhibit broadening of the Spalt, the DPP direct target, domain. Wild-type wing imaginal discs (A-D) or wing imaginal disc with large *how^{stru}* mutant clones (E-H) stained for HOW (red; A,E), Spalt (green; B,F) and Engrailed (blue; C,G). (D,H) Merged images of HOW (red) and Spalt (green) expression. Arrowheads indicate the anteroposterior boundary. (I) Quantification of the Spalt (Sal) domain width in wild-type (WT) or in mutant (CLONES) discs is given as the ratio between a cumulative value representing Spalt width (in upper, lower and middle regions) and the wing imaginal disc width (Sal/disc).

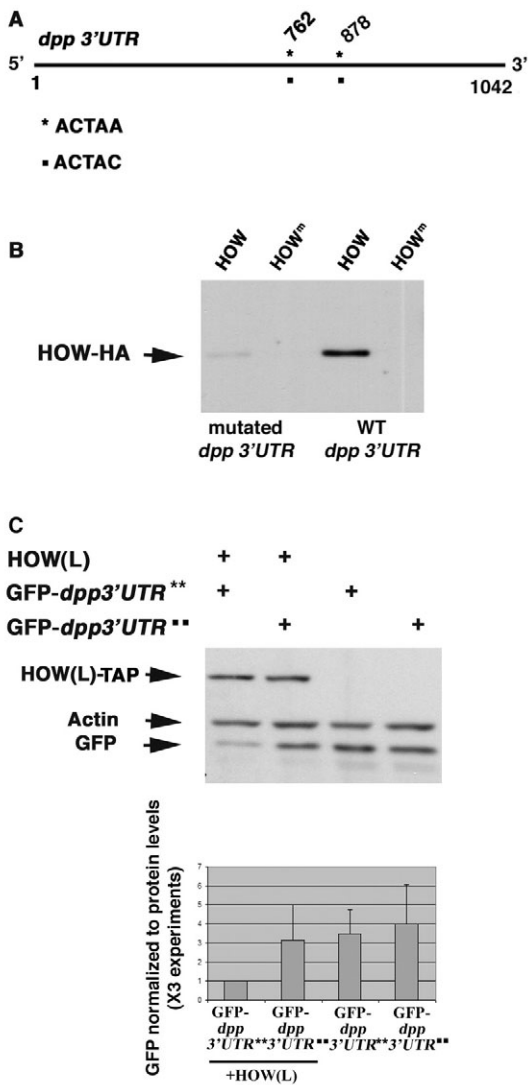


Fig. 3. Two HRE sites in the *dpp* 3'UTR mediate the binding and repression of HOW. (A) Schematic representation of the two HRE sites in the 3'UTR of *dpp*. These sites were mutated as described. (*) Wild-type sequences; (■) mutated sequence. (B) Western blot analysis for HA-tagged HOW or HOW^m (HOW-HA) following precipitation with the wild-type (WT) or mutated *dpp* 3'UTR. (C) Western blot analysis with anti-GFP, anti-actin and anti-TAP of S-2R+ cells transfected with GFP-*dpp*3'UTR containing wild-type or mutated HRE sites, together with or in the absence of HOW(L). The bar graph represents the results of three independent transfection experiments that were normalized to the actin levels of each sample.

(Fig. 3C). Transfection of S-2R+ cells with HOW(L)-TAP together with either GFP-*dpp*3'UTR or mutated GFP-*dpp*3'UTR, which lacks the HREs, was followed by western blot analysis with anti-GFP. In the presence of HOW(L), the GFP-DPP3'UTR levels were reduced threefold (after normalization to actin levels) relative to the levels of GFP-DPP3'UTR lacking the HREs. S-2R+ cells that did not overexpress HOW(L) did not show a significant difference in the GFP levels between the two constructs (Fig. 3C). For comparison, the levels of GFP-Stripe3'UTR were reduced around sixfold when combined with HOW(L) in S2R+ cells. This reduction was apparent also in the RNA levels of the GFP-*dpp*3'UTR construct as measured by reverse transcriptase (RT)-

PCR (data not shown). These experiments demonstrate that HOW(L) exhibits repressive activity upon binding to the HRE sites in *dpp* 3'UTR.

HOW(L) is highly expressed in the wing imaginal disc. To test its effect on *dpp* mRNA in the wing imaginal disc, we induced the expression of HOW(L) together with a construct of *dpp*-GFP fusion that either contained, or lacked the *dpp* 3'UTR sequence (Entchev et al., 2000; Teleman and Cohen, 2000). Both the *UAS-how(L)* and the *UAS-dpp-gfp* constructs were driven by the *vestigial-gal4* driver, which is expressed along the dorsoventral boundary of the wing imaginal disc. We noticed a consistent and significant HOW(L)-dependent reduction of the level of DPP-GFP only when this construct contained the *dpp* 3'UTR (Fig. 4A,D,G,J). Interestingly, the HOW(L)-mediated repression was detected mostly in the wing pouch region of the wing imaginal disc region and not in the more distal parts of the imaginal disc, possibly indicating additional control of HOW(L) activity in this domain. Thus, HOW(L) represses DPP-GFP levels not only in S-2R+ cells but also in vivo in the wing imaginal disc, presumably via its direct association with the *dpp* 3'UTR.

HOW(L) affects the Spalt domain non-autonomously

Consistent with the effect of HOW(L) on the production of the DPP-GFP protein construct, we observed a significant reduction of the Spalt domain following overexpression of HOW(L) in the wing imaginal disc pouch using the *sd-gal4* driver (Fig. 5A,H).

If HOW(L) affects the Spalt domain indirectly by repressing endogenous *dpp* mRNA levels, its effect should be non-autonomous, because DPP protein diffuses distally from the anteroposterior border. To differentiate between an autonomous versus non-autonomous effect of HOW on the Spalt expression domain, we overexpressed HOW(L) within the DPP domain using the *dpp-gal4* driver. This resulted in a reduction of the Spalt domain beyond the HOW(L) expression domain (compare the Spalt domain in Fig. 5E with that in 5H). Importantly, in quantitative analysis of the Spalt-expressing cells in the HOW(L)-overexpressing imaginal disc, the posterior compartment (where DPP is not expressed) showed a 20% reduction of this domain (calculated as in Fig. 2), indicating a non-autonomous effect of HOW(L) (Fig. 5I). These results are consistent with HOW affecting the levels of the diffusing DPP morphogen. A control experiment driving HOW(L) with *hedgehog-gal4* (expressed in the posterior compartment) did not reduce the Spalt domain, nor did it have any effect on cell viability [as measured by active Caspase 3 (also known as DEWAY) staining (data not shown)].

To test directly whether HOW(L) is capable of reducing *dpp* mRNA levels, we performed in situ analysis with a *dpp* probe on the wing imaginal discs expressing ectopic HOW(L) by the *sd-gal4* driver. The results indicate a significant decrease in *dpp* mRNA in the *sd-gal4* expression domain (Fig. 5J,K). Taken together, these results demonstrate that ectopically expressed HOW(L) can repress *dpp* mRNA levels.

Reduction of endogenous HOW levels leads to an elevation of endogenous *dpp* mRNA

To test further the contribution of HOW to the reduction of endogenous *dpp* mRNA levels, we reduced the levels of the HOW(L) isoform, or the levels of all HOW isoforms, using dsRNA complementary to HOW(L), or to a part of the HOW coding sequence shared by all isoforms, driven by the *sd-gal4* driver. We detected a significant elevation of *dpp* mRNA in the wing imaginal disc pouch, where the *sd-gal4* is highly expressed in both cases (Fig.

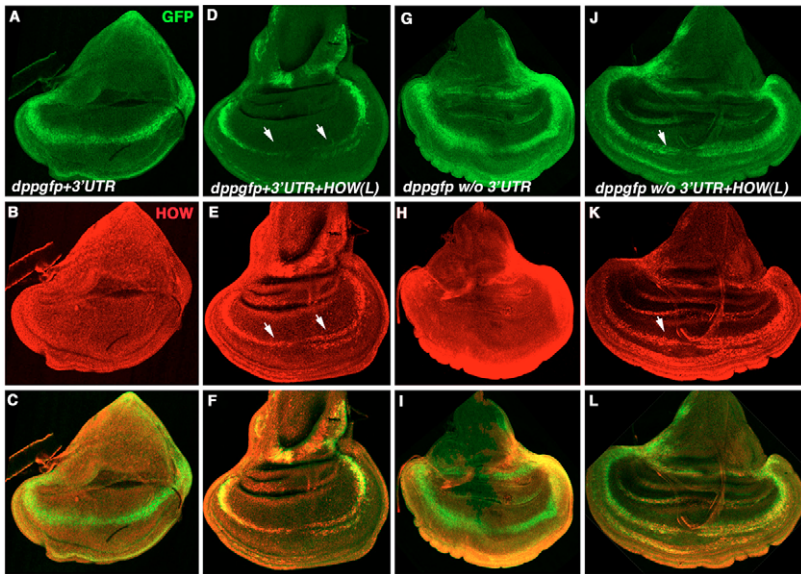


Fig. 4. HOW(L) represses the levels of DPP-GFP in a 3'UTR-dependent manner. (A-L) Wing imaginal discs labeled with GFP (A,D,G,J) or with anti-HOW (red; B,E,H,K) were dissected from larvae carrying the *vestigial-gal4* driver and UAS-HOW(L) (D-F,J-L), and either a *dpp-GFP* fusion construct that contains the *dpp* 3'UTR (A-F) or one lacking the *dpp* 3'UTR (G-L). The corresponding merged panels are shown (C,F,I,L). Arrows show reduced GFP expression in the presence of HOW(L) and *dpp* 3'UTR, and normal GFP expression in the absence of the 3'UTR of *dpp*. Note a significant reduction of DPP-GFP in the presence of HOW(L) only when the *dpp-GFP* construct contains the endogenous *dpp* 3'UTR (D).

6B,C). Accordingly, we detected a reduction in HOW protein levels in the *sd-gal4* expression domain in both cases (Fig. 6D,G). Targeted expression of HOW(L), or of HOW dsRNA (using *sd-gal4*), phenocopied the *how* mutant blistered phenotype in the adult wing (Fig. 6K,L), supporting the relevance of these dsRNA constructs to HOW function. We also found that a continuous expression of dsRNA corresponding to the HOW(L) isoform in the pupal wing using the *ms1096-gal4* driver led to the formation of ectopic veins in 100% ($n=60$) of the wings (Fig. 6N). This phenotype was observed only with *how(L)*-specific dsRNA. Such a phenotype is observed following the overexpression of DPP in the pupal wing (Bangi and Wharton, 2006).

These results demonstrate that HOW functions to suppress endogenous *dpp* mRNA levels in the wing imaginal disc and pupal wing.

DISCUSSION

Accumulating data regarding the activity of STAR proteins suggest that they regulate an array of target mRNA species required for tissue differentiation in a spatial and temporal fashion (Kuersten and Goodwin, 2003; Lasko, 2003; Larocque and Richard, 2005; Vernet and Artzt, 1997). This study characterized the HOW response element (HRE) both at the level of primary sequence and of secondary structure. Although the primary sequence is closely related to that of the published response sequences of quaking and Gld-1, suggesting that STAR proteins share binding specificity, our study adds an important additional aspect: the secondary-structure restrictions that regulate the binding of HOW, quaking and, presumably, other STAR proteins to the primary response element sequence. These restrictions may help to further select for active HREs from the multiple sequences containing the relatively

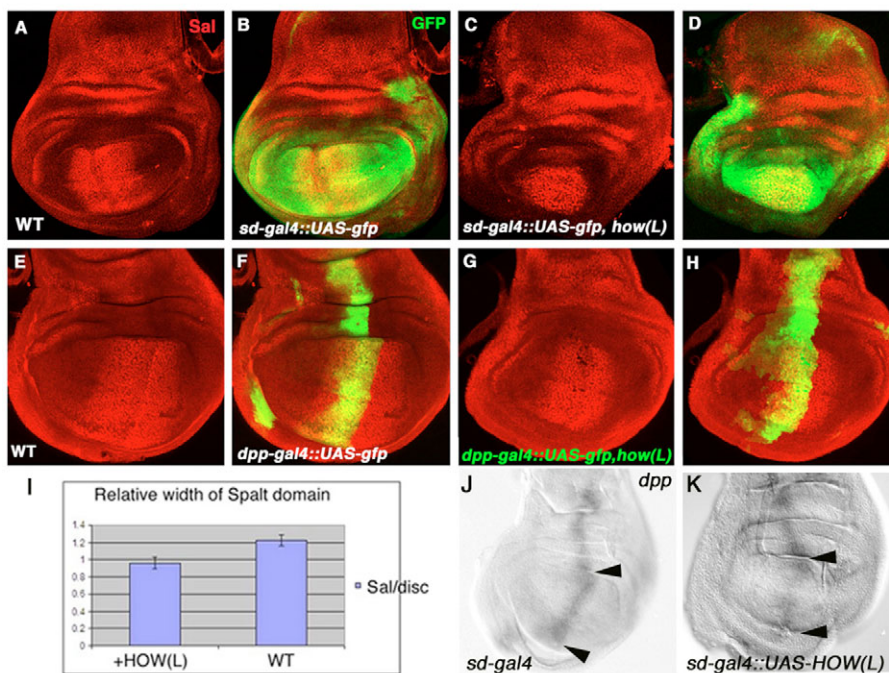


Fig. 5. Overexpression of HOW(L) reduces the Spalt domain non-autonomously and represses *dpp* mRNA expression.

(A-H) Wing imaginal discs carrying *sd-gal4* (A-D) or *dpp-gal4* (E-H) and either UAS-GFP alone (A,B,E,F) or together with the repressor isoform UAS-HOW(L) (C,D,G,H) stained for Spalt (Sal, red). The merged images of GFP and Spalt are shown (B,D,F,H).

(I) Quantification of the Spalt domain width in wild type (WT) and in wing imaginal discs overexpressing HOW(L) in the *dpp* domain is given as the ratio between Spalt domain width and the wing imaginal disc width (calculated as detailed in Fig. 2). (J,K) In situ hybridization with the DIG-labeled *dpp* antisense probe of wing imaginal discs carrying *sd-gal4* (J), or overexpressing HOW(L) driven by the *sd-gal4* driver (K). Arrowheads indicate the wing imaginal disc pouch domain.

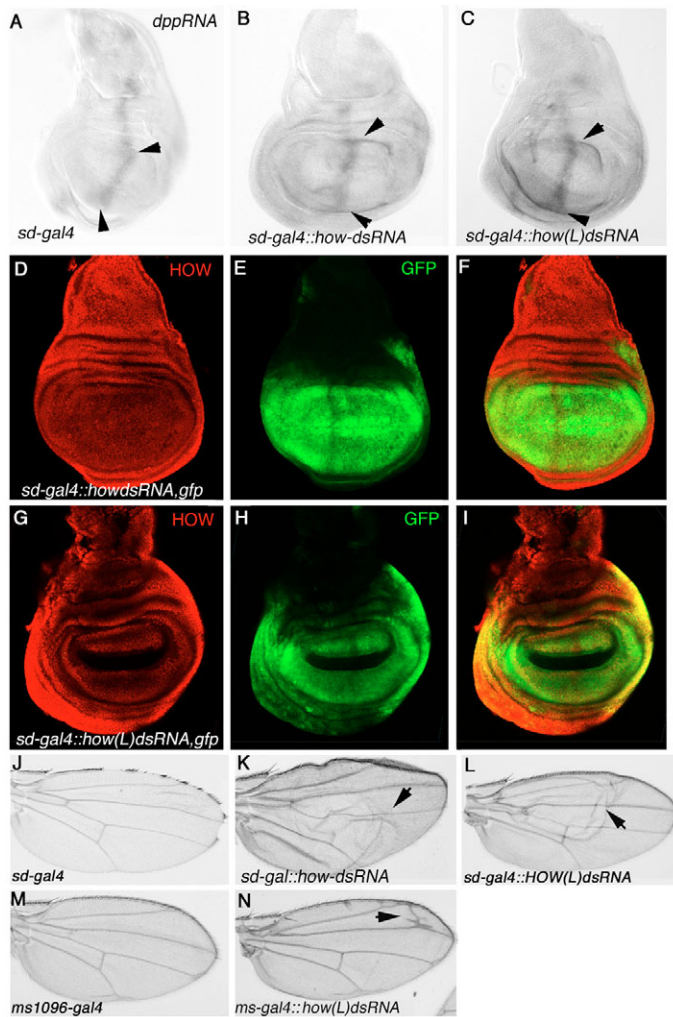


Fig. 6. Reduction of HOW levels elevates endogenous *dpp* mRNA. (A-C) In situ hybridization of wing imaginal discs with a *dpp*-specific probe carrying the *sd-gal4* driver alone (A), or together with *how*-specific dsRNA (B) or with *how(L)*-specific dsRNA (C). Arrowheads indicate the *sd*-expression domain. Notice the specific elevation of *dpp* in the wing imaginal disc pouch in B and C. (D-I) Wing imaginal discs carrying the *sd-gal4* driver and *UAS-GFP* together with *how*-specific dsRNA (D,E,F) or together with *how(L)*-specific dsRNA (G,H,I) stained for anti-HOW (D,G) and labeled with GFP (E,H). Their corresponding merged images are shown in F and I. Notice the specific reduction of HOW in the *sd-gal4* expression domain in both D and G. (J-L) Adult wings of flies carrying the *sd-gal4* driver alone (J), or in combination with *how*-specific dsRNA (K) or with *how(L)*-specific dsRNA (L). Arrows point to wing blisters. (M,N) Adult wings of flies carrying the *ms1096-gal4* alone (M) or together with *how(L)*-specific dsRNA (N). Arrow points to extra veins.

abundant pentamer. However, because, in many cases, determination of the actual secondary structure of a given 3'UTR is not definitive, further experiments are often required to define an actual HOW target mRNA.

An ongoing study in our laboratory characterizing HOW mRNA targets in the embryonic mesoderm strongly supports the structural requirements identified here (Toledano-Katchalsky et al., unpublished). In all cases tested, HREs within the 3'UTRs of genes that are predicted to be embedded within a large loop showed HOW-specific binding.

Our structural studies helped us to identify a novel HOW target, namely *dpp* mRNA, in the wing imaginal disc. We suggest that, normally, the repressor isoform of HOW, HOW(L), reduces *dpp* mRNA levels in the wing imaginal disc and in the pupal wing, leading to reduced DPP protein levels during the establishment of the anteroposterior axis, and later during wing vein formation. Presumably, in the absence of HOW(L), higher DPP levels at the source would alter the overall shape of the DPP gradient, thus expanding the Spalt expression domain. The phenotype of ectopic veins obtained by continuous expression of HOW(L) dsRNA in the pupal wings supports an additional role for HOW(L) in repressing *dpp* mRNA at later stages of wing development.

The sensitivity of the embryo to DPP levels has been demonstrated by the DPP haplo-insufficient phenotype (Podos and Ferguson, 1999). This sensitivity is also exhibited in the wing imaginal disc by the observation that endogenous *dpp* can be replaced by *UAS-GFP-dpp* driven by *dpp-gal4* only at low temperatures [16°C (Entchev et al., 2000) or 19°C (Teleman and Cohen, 2000)], at which the Gal4 protein is significantly less active. Because the responsiveness of the cells to DPP levels is highly sensitive, it is necessary to tightly regulate the levels of DPP protein; for example, by constitutive reduction of its mRNA levels in DPP-secreting cells by the HOW(L) protein.

In summary, we have elucidated the primary- and secondary-structure requirements for the binding of HOW to its target mRNA. This will facilitate the identification of novel targets for STAR proteins in other species. Importantly, our analysis uncovered a novel post-transcriptional mechanism that regulates *dpp* mRNA levels in the wing imaginal disc

We thank O. Gerlitz (Hebrew University), S. Cohen (EMBL), M. Gozalez-Gaitan (MPI, Dresden), K. Basler (Zurich University), A. Salzberg (Technion, Haifa), the Hybridoma Stock Center and the Bloomington Stock Center for various fly lines and antibodies; and Z. Paroush, B. Shilo, S. Michaeli, S. Schwarzbaum and members of the Volk laboratory for their critical reading of the manuscript. This work was supported by a grant from the Israel Science Foundation (ISF).

References

- Baehrecke, E. H. (1997). who encodes a KH RNA binding protein that functions in muscle development. *Development* **124**, 1323-1332.
- Bangi, E. and Wharton, K. (2006). Dual function of the Drosophila Alk1/Alk2 ortholog Saxophone shapes the Bmp activity gradient in the wing imaginal disc. *Development* **133**, 3295-3303.
- Crittenden, S. L., Eckmann, C. R., Wang, L., Bernstein, D. S., Wickens, M. and Kimble, J. (2003). Regulation of the mitosis/meiosis decision in the Caenorhabditis elegans germline. *Philos. Trans. R. Soc. Lond. B Biol. Sci.* **358**, 1359-1362.
- de Moor, C. H., Meijer, H. and Lissenden, S. (2005). Mechanisms of translational control by the 3' UTR in development and differentiation. *Semin. Cell Dev. Biol.* **16**, 49-58.
- Ebersole, T. A., Chen, Q., Justice, M. J. and Artzt, K. (1996). The quaking gene product necessary in embryogenesis and myelination combines features of RNA binding and signal transduction proteins. *Nat. Genet.* **12**, 260-265.
- Entchev, E. V., Schwabedissen, A. and Gonzalez-Gaitan, M. (2000). Gradient formation of the TGF-beta homolog Dpp. *Cell* **103**, 981-991.
- Galarneau, A. and Richard, S. (2005). Target RNA motif and target mRNAs of the Quaking STAR protein. *Nat. Struct. Mol. Biol.* **12**, 691-698.
- Kuersten, S. and Goodwin, E. B. (2003). The power of the 3' UTR: translational control and development. *Nat. Rev. Genet.* **4**, 626-637.
- Larocque, D. and Richard, S. (2005) QUAKING KH domain proteins as regulators of glial cell fate and myelination. *RNA Biol.* **2**, 37-40.
- Lasko, P. (2003). Gene regulation at the RNA layer: RNA binding proteins in intercellular signaling networks. *Sci. STKE* **2003**, RE6.
- Lee, M. H. and Schedl, T. (2001). Identification of in vivo mRNA targets of GLD-1, a maxi-KH motif containing protein required for C. elegans germ cell development. *Genes Dev.* **15**, 2408-2420.
- Li, Z., Zhang, Y., Li, D. and Feng Y. (2000). Destabilization and mislocalization of myelin basic protein mRNAs in quaking dysmyelination lacking the QKI RNA-binding proteins. *J. Neurosci.* **20**, 4944-4953.
- Lo, P. C. and Frasch, M. (1997). A novel KH-domain protein mediates cell adhesion processes in Drosophila. *Dev. Biol.* **190**, 241-256.

- Mathews, D. H., Sabina, J., Zuker, M. and Turner, D. H.** (1999). Expanded sequence dependence of thermodynamic parameters improves prediction of RNA secondary structure. *J. Mol. Biol.* **288**, 911-940.
- Nabel-Rosen, H., Dorevitch, N., Reuveny, A. and Volk, T.** (1999). The balance between two isoforms of the Drosophila RNA-binding protein how controls tendon cell differentiation. *Mol. Cell* **4**, 573-584.
- Nabel-Rosen, H., Volohonsky, G., Reuveny, A., Zaidel-Bar, R. and Volk, T.** (2002). Two isoforms of the Drosophila RNA binding protein, how, act in opposing directions to regulate tendon cell differentiation. *Dev. Cell* **2**, 183-193.
- Nabel-Rosen, H., Toledano-Katchalski, H., Volohonsky, G. and Volk, T.** (2005). Cell divisions in the drosophila embryonic mesoderm are repressed via posttranscriptional regulation of string/cdc25 by HOW. *Curr. Biol.* **15**, 295-302.
- Podos, S. D. and Ferguson, E. L.** (1999). Morphogen gradients: new insights from DPP. *Trends Genet.* **15**, 396-402.
- Prout, M., Damania, Z., Soong, J., Fristrom, D. and Fristrom, J. W.** (1997). Autosomal mutations affecting adhesion between wing surfaces in Drosophila melanogaster. *Genetics* **146**, 275-285.
- Ryder, S. P. and Williamson, J. R.** (2004). Specificity of the STAR/GSG domain protein Qk1: implications for the regulation of myelination. *RNA* **10**, 1449-1458.
- Ryder, S. P., Frater, L. A., Abramovitz, D. L., Goodwin, E. B. and Williamson, J. R.** (2004). RNA target specificity of the STAR/GSG domain post-transcriptional regulatory protein GLD-1. *Nat. Struct. Mol. Biol.* **11**, 20-28.
- Teleman, A. A. and Cohen, S. M.** (2000). Dpp gradient formation in the Drosophila wing imaginal disc. *Cell* **103**, 971-980.
- Vernet, C. and Artzt, K.** (1997). STAR, a gene family involved in signal transduction and activation of RNA. *Trends Genet.* **13**, 479-484.
- Zaffran, S., Astier, M., Gratecos, D. and Semeriva, M.** (1997). The held out wings (how) Drosophila gene encodes a putative RNA-binding protein involved in the control of muscular and cardiac activity. *Development* **124**, 2087-2098.
- Zuker, M.** (2003). Mfold web server for nucleic acid folding and hybridization prediction. *Nucleic Acids Res.* **31**, 3406-3415.